ACS Energy LETTERS

http://pubs.acs.org/journal/aelccp

REVIEW

Sulfide-Based Anode-Free Solid-State Batteries: Key Challenges and Emerging Solutions

Jiwei Wang and Hongli Zhu*

Cite This: ACS Energy Lett. 2025, 10, 2377−2391

Read Online

ACCESS | Metrics & More | Article Recommendations

ABSTRACT: Sulfide-based anode-free solid-state batteries (AFSSBs) have emerged as a transformative technology for next-generation energy storage, offering compelling advantages in energy density, safety, and manufacturing scalability. However, these batteries face significant challenges, particularly rapid capacity degradation that currently limits their practical implementation. This comprehensive review critically examines three fundamental issues affecting AFSSBs: nonuniform lithium nucleation on bare current collectors, unstable interfaces between plated lithium and sulfide electrolytes, and formation of interfacial voids during cycling. We systematically evaluate recent strategic advances in addressing these challenges, including metal seed coatings, conversion reaction-based compounds, and carbon-based interlayers. The review also analyzes the crucial role of advanced characterization techniques, from cryo-FIB-SEM to operando methods, in understanding failure mechanisms and validating improvement strategies. Finally, we present a forward-looking perspective on research directions necessary for commercialization. This work provides a thorough framework for understanding and advancing sulfide-based AFSSBs toward practical applications in next-generation energy storage systems.

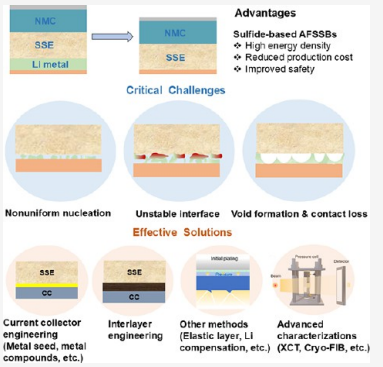

The transition to sustainable energy systems has significantly accelerated the demand for advanced energy storage technologies with high energy density, long cycle life, and enhanced safety.[1,2] Over the past 30 years, commercial lithium-ion batteries (LIBs) with graphite anodes have dominated the energy storage market.[3,4] However, their energy density is fundamentally constrained by the low specific capacity of graphite (~372 mAh g^{-1}), leading to a cell-level energy density of approximately 250 Wh kg^{-1} (Figure 1).[5] This limitation is insufficient to meet the increasing energy density requirements for next-generation electric vehicles (EVs), which demand extended driving ranges and faster charging capabilities.[6]

To overcome these limitations, lithium (Li) metal anodes have been identified as a promising alternative due to their ultrahigh theoretical specific capacity (3860 mAh g^{-1}) and the lowest electrochemical potential (−3.04 V vs standard hydrogen electrode) among all known anode materials.[7,8] By coupling Li metal anodes with solid electrolytes (SEs), all-solid-state lithium metal batteries (ASSLMBs) have emerged as a next-generation energy storage technology, offering superior energy density, enhanced safety, and thermal stability compared to conventional LIBs (Figure 1).[9] Among various SEs, sulfide-based SEs (e.g., Li_6PS_5Cl (LPSC), $Li_{10}GeP_2S_{12}$)

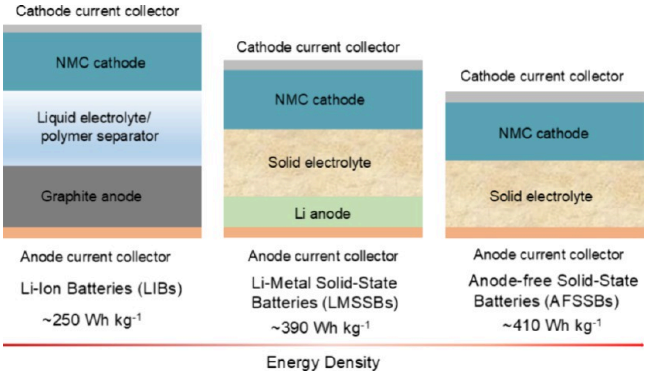

Figure 1. Schematic representation and comparison of commercial Li-Ion batteries (LIBs), Li-metal solid-state batteries (LMSSBs), and anode-free solid-state batteries (AFSSBs).

Received: February 17, 2025
Revised: April 2, 2025
Accepted: April 7, 2025

have attracted particular attention due to their exceptional ionic conductivity at room temperature ($\sim 10^{-2}$ S·cm^{-1}) and favorable mechanical properties, which enable intimate contact with electrode materials and low interfacial resistance.[10,11] Despite these advantages, sulfide-based ASSLMBs face a series of practical challenges including the high cost and complexity of fabricating thin Li metal anodes, uncontrolled Li dendrite growth leading to penetration through solid electrolyte, and severe interfacial instability caused by the chemical reduction of sulfide-based SEs upon contact with reactive Li metal.[12−14] These issues not only compromise cycling stability but also hinder large-scale commercialization.

To further enhance the energy density and simplify the manufacturing process, **anode-free solid-state batteries (AFSSBs)** have recently emerged as a promising alternative to conventional ASSLMBs (Figure 1).[15,16] In AFSSBs, a bare current collector (CC) replaces the predeposited Li metal anode. During the initial charge, Li ions are electrochemically extracted from the cathode and plated in situ onto the CC. During discharge, the plated Li is stripped and reinserted into the cathode. This unique configuration offers several significant advantages: (1) the elimination of preloaded Li metal minimizes the weight and volume of the cell, resulting in higher gravimetric and volumetric energy densities; (2) the need for thin Li metal fabrication is eliminated, simplifying the manufacturing process, reducing production costs, and enhancing scalability for commercial applications; and (3) improved safety due to the elimination of highly reactive metallic Li during manufacturing.

However, while AFSSBs demonstrate significant potential, sulfide-based AFSSBs face critical challenges that must be addressed to achieve practical performance. First, the uncontrolled Li deposition on bare metal CCs leads to nonuniform Li plating, which promotes dendrite formation and dead Li, ultimately causing rapid capacity decay. Second, the high reactivity between plated Li and sulfide SEs results in interfacial instability, exacerbating resistance buildup and structural degradation. Third, the limited Li source in AFSSBs intensifies these challenges compared to conventional ASSLMBs with excess Li reservoirs, further restricting the cycle life and reliability of the batteries. To address these challenges, numerous strategies have been developed, including current collector modification, interlayer engineering, cathode prelithiation, and electrolyte engineering, for achieving remarkable performance improvement.[17−22] A recent perspective provides an overview of key factors influencing the performance of AFSSBs and highlights some of the strategies, such as interlayer engineering and current collector modification, for performance enhancement.[23]

Despite significant progress, a comprehensive review specifically focused on sulfide-based AFSSBs remains rare. Given the increasing research efforts in this field, it is essential to consolidate recent advancements, identify key challenges, and outline future opportunities to guide the rational design of high-performance sulfide-based AFSSBs. This review aims to provide a detailed overview of the current issues and advancements in sulfide-based AFSSBs. We first discuss the challenges and limitations associated with sulfide-based AFSSBs. Next, we summarize various strategies to enhance the performance of sulfide-based AFSSBs. Furthermore, advanced ex situ and in situ/operando characterization techniques are reviewed to diagnose the failure mechanisms of sulfide-based AFSSBs. Finally, future perspectives are proposed to offer insights and ideas for the practical development of high-performance sulfide-based AFSSBs.

CRITICAL CHALLENGES OF SULFIDE-BASED AFSSBS

Since the anode-free concept was proposed to overcome the energy density limitations of traditional LIBs, sulfide-based AFSSBs have emerged as one of the most promising energy storage technologies due to their numerous advantages, such as higher energy density, improved safety, lower fabrication costs, and simplified manufacturing processes. However, sulfide-based AFSSBs suffer from rapid capacity degradation, which significantly hinders their practical application. Therefore, a fundamental understanding of their failure mechanisms and the associated challenges is imperative for achieving long-term cycling stability.

In sulfide-based AFSSBs, Li is directly plated onto the bare CC rather than pre-existing metallic Li. However, due to the inherent surface properties of the CC, which often exhibit poor Li wettability, Li plating on CC in AFSSBs typically requires overcoming a higher nucleation energy barrier compared to preloaded lithium metal.[17,24−27] Consequently, Li nucleation on bare CC tends to be nonuniform, leading to uneven Li deposition during the initial charging process (Figure 2A). In

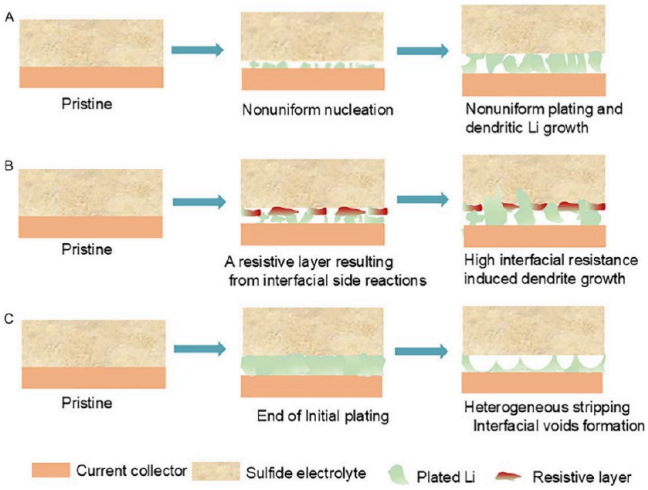

Figure 2. Schematic illustration of issues affecting the cycling performance of sulfide-based AFSSBs. (A) Nonuniform Li nucleation. (B) Unstable interface between plated Li and SE. (C) Interfacial voids formation at the end of stripping.

subsequent cycles, this uneven deposition promotes Li dendrite growth and the formation of dead Li, ultimately resulting in poor plating/stripping efficiency and rapid capacity degradation. To mitigate this issue, surface modifications of the CC or the introduction of lithophilic metal seeds are thus proposed as promising strategies to facilitate uniform Li deposition.

Although sulfide SEs offer higher ionic conductivity than their oxide or polymer counterparts, they suffer from poor chemical and electrochemical stability against Li metal. Sulfide SEs are prone to reduction at low potentials, forming interphases with low ionic conductivity.[28−32] These interphases significantly increase interfacial resistance, leading to sluggish Li^+ diffusion at the anode/SE interface and uneven Li^+ flux near the CC surface (Figure 2B). Consequently, the elevated interfacial resistance accelerates Li dendrite growth.

https://doi.org/10.1021/acsenergylett.5c00517
ACS Energy Lett. 2025, 10, 2377−2391

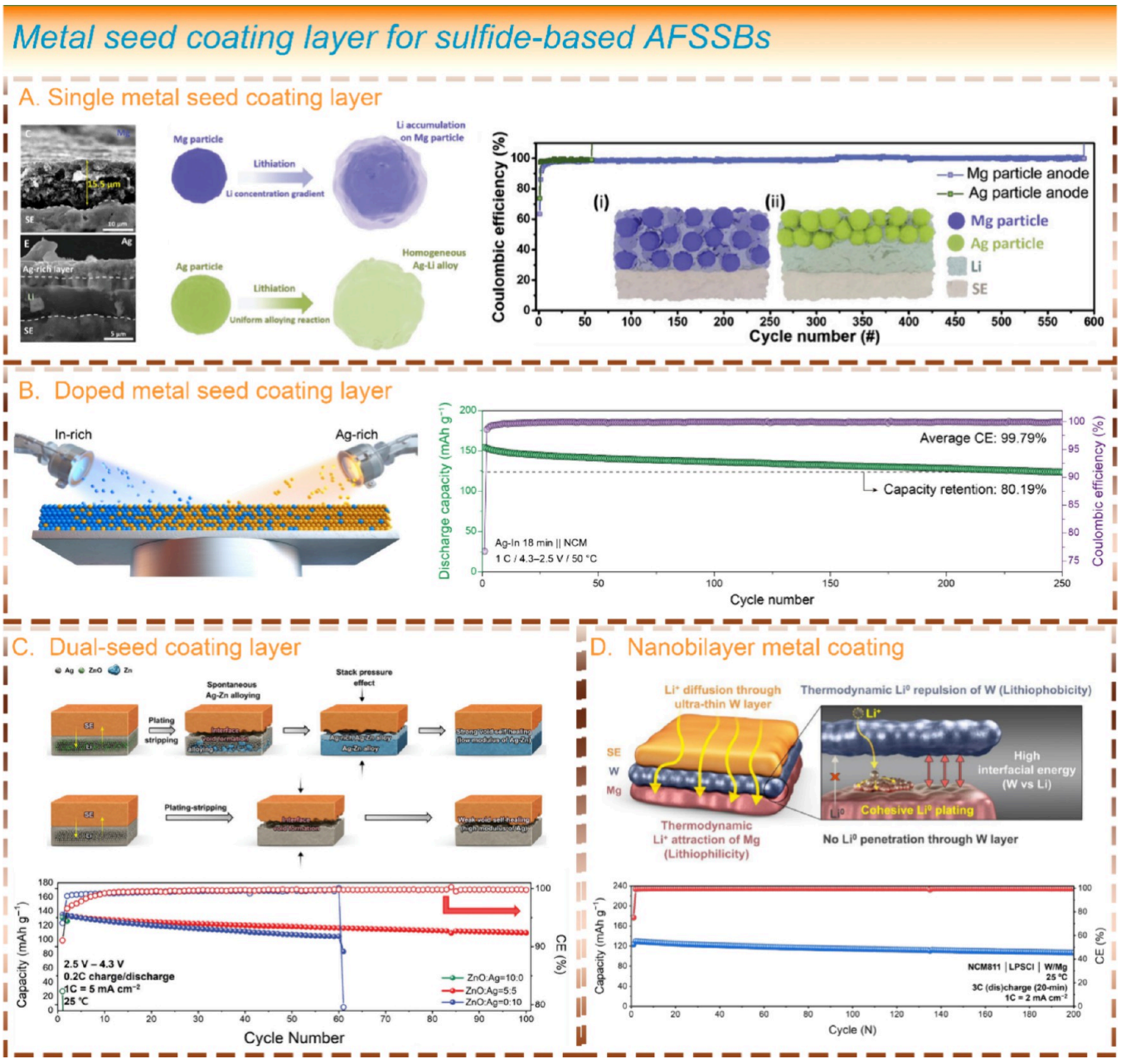

Figure 3. (A) Cross-sectional SEM images of the Mg and Ag particle anodes after Li deposition of 2 mAh cm^{-2}. Schematic illustration of lithiation process of Mg and Ag particles. Coulombic efficiency comparison of Mg and Ag particle anodes in half cells. The current density was 0.5 mA cm^{-2} with a fixed capacity of 2 mAh cm^{-2}. Reproduced with permission from ref 40. Copyright 2023 Wiley-VCH. (B) Schematic illustration of Ag−In coated current collector through a sputtering method. Cycling performance of full cell with In-doped Ag seed tested at 50 °C. Reproduced with permission from ref 41. Copyright 2024 Elsevier. (C) Schematic of Ag single-seed and Ag-ZnO dual seed for stabilizing the anode-free interfaces. Cycling performance comparison of the anode-free full cells with Ag-ZnO, ZnO, and Ag seeds. Reproduced with permission from ref 43. Copyright 2024 Wiley-VCH. (D) Schematic illustration of the charging process with W/Mg nanobilayer coating. Cycling performance of the anode-free full cell with W/Mg nanobilayer coating tested at 25 °C. Reproduced with permission from ref 44. Copyright 2024 Royal Society of Chemistry.

Additionally, the limited Li reservoir in AFSSBs exacerbates the problem, as parasitic reactions consume active Li, which cannot be replenished, unlike in LMBs. Thus, suppressing interfacial reactions is critical for enabling the long-term cycling stability of sulfide-based AFSSBs. Potential strategies include the development of stable interlayers or optimizing electrolyte formulations to minimize parasitic reactions.

Another critical challenge in sulfide-based AFSSBs is the formation of interfacial voids due to the heterogeneous stripping, which leads to low plating/stripping efficiency and rapid capacity degradation. Li plating and stripping on the CC induce significant volume changes at the solid−solid interface. When Li is irregularly deposited, interfacial voids can easily form at the end of the stripping process, resulting in contact loss between the CC and the SE (Figure 2C).[33−36] Furthermore, unlike Li metal anode, which is relatively soft and can deform to maintain good interfacial contact, the metallic CC foil used in AFSSBs is rigid, which limits its ability

https://doi.org/10.1021/acsenergylett.5c00517
ACS Energy Lett. 2025, 10, 2377−2391

to accommodate the interfacial stress, exacerbating contact loss at the interface. These interfacial voids and contact losses disrupt ionic and electronic pathways, increasing interfacial resistance. Additionally, they can isolate active Li, leading to dead Li formation and causing irreversible capacity loss. Addressing this issue requires engineering compliant interfacial layers or adopting advanced CC designs that can accommodate volume changes more effectively, thereby maintaining continuous contact with the SE and mitigating void formation.

STRATEGIES FOR IMPROVING THE PERFORMANCE OF SULFIDE-BASED AFSSBS

Sulfide-based AFSSBs face several critical challenges, including uncontrolled Li growth and inferior Li plating/stripping efficiency. These issues arise from nonuniform Li nucleation on the bare lithophobic current collector and parasitic reactions between Li and the SE, leading to rapid capacity decay. Moreover, compared to the sulfide-based LMBs with excess Li, the limited Li reservoir in AFSSBs exacerbates the issues of uneven Li deposition and low plating/stripping Coulombic efficiency (CE), making it even more challenging to achieve long-term cycling stability. Therefore, addressing these challenges is crucial for developing high performance and long-lifetime sulfide-based AFSSBs. To date, various strategies have been proposed to enhance the electrochemical performance of sulfide-based AFSSBs, which can be broadly classified into the following approaches: (1) metal seed coating layer; (2) conversion reaction-based metal compound layer; (3) interlayer designs; (4) other methods.

METAL SEED COATING LAYER

The electrochemical deposition of Li directly onto the bare CC suffers from inhomogeneous nucleation and growth due to the high Li nucleation energy barrier and the lack of favorable surface interactions, leading to localized Li accumulation and uneven stress distribution at the interface. Lithophilic metal seed coatings on the CC have emerged as a promising strategy to solve these challenges.[37−39] The lithophilic metal seeds act as predesigned nucleation sites with a lower energy barrier for Li deposition, enabling uniform nucleation across the CC's surface and promoting controlled Li growth. Moreover, metal seed coatings can alleviate the mechanical and electrochemical issues associated with Li deposition in sulfide-based AFSSBs. By promoting uniform growth of Li, metal seed coatings can suppress the formation of high-surface-area dendritic Li, which is susceptible to undesirable side reactions with sulfide SE. Consequently, the interfacial contact becomes more intimate during the stripping process, which could improve the CE and extend the cycle lifetime.

For instance, Lee et al.[40] studied the use of Mg and Ag particles as lithiphilic metal seeds to modify CCs and examined their effects on Li deposition in sulfide-based AFSSBs (Figure 3A). They found that Li deposition behavior differed significantly between the two coatings. For Mg particles, Li accumulated primarily between the particles rather than at the Mg/solid electrolyte (SE) interface. This was attributed to the slow alloying kinetics of Mg with Li and sluggish Li diffusion within the Li−Mg alloy, which created a Li concentration gradient that attracted Li to the particle surface. In contrast, Ag particles exhibited fast lithiation and rapid Li diffusion in the Li−Ag alloy, resulting in a uniform Li distribution within the alloy. This caused volume expansion and reduced porosity, limiting Li penetration into pores and confining deposition to the Li−Ag/SE interface. While both seeds promoted uniform Li deposition, Mg particles provided superior cycle stability by suppressing delamination between the anode and SE due to the Li deposits between Mg particles. Later, Yu et al.[41] demonstrated that doping a small amount of indium (In) into an Ag lithophilic metal coating layer on a stainless steel (SS) CC significantly enhances the performance of sulfide-based AFSSBs compared to a pure Ag seed coating layer (Figure 3B). This improvement is attributed to two key factors: (1) In doping increases Li adsorption energy and reduces diffusion barriers, thereby facilitating Li transfer within the Ag coating layer; and (2) In doping induces the formation of an In−S interfacial layer at the SE/coating layer interface, which stabilizes the interface.[42] As a result, the Ag−In/NMC full cell exhibited a remarkable improvement in cycling stability, retaining 80.2% of its capacity after 250 cycles. This study suggests that single-metal seed coating layers may not fully satisfy all the requirements for achieving high-performance sulfide-based AFSSBs.

To overcome these limitations, Choi et al.[43] proposed a dual-seed coating layer comprising Ag and ZnO nanoparticles to enhance the performance of sulfide-based AFSSBs (Figure 3C). The dual-seed structure facilitates Li diffusion through multistep lithiation pathways due to the distinct lithiation potentials of Ag and ZnO. Additionally, the Zn−Ag alloy mitigates interfacial voids during stripping, as the alloy exhibits greater softness and ductility compared to a single Ag seed. These features enable the Ag−Zn dual-seed full cell to achieve a high-capacity retention of 80.8% after 100 cycles at 1 mA cm^{-2} and 3 mAh cm^{-2} at room temperature. Despite these advantages, the long-term performance of the dual-seed structure remains suboptimal. To further improve performance, Choi et al.[44] introduced a thin nanobilayer coating strategy, where a lithophobic tungsten (W) layer is deposited on a lithophilic Mg layer. The lithophobic W layer suppresses Li dendrite growth due to its high interfacial energy, while the lithophilic Mg layer promotes uniform Li nucleation and deposition. This synergistic effect of the nanobilayer coating significantly enhances the full cell's performance (Figure 3D).

CONVERSION REACTION-BASED METAL COMPOUNDS LAYER

Although metal seed coatings show great promise in promoting uniform Li plating by reducing nucleation energy barriers, they face significant challenges in stabilizing sulfide-based AFSSBs. For example, metal coating layers are susceptible to deformation or delamination under repeated Li plating/stripping cycles due to the substantial volume changes of Li. Additionally, these coatings often fail to prevent interfacial degradation as they do not inhibit the chemical or electrochemical interactions between Li and the SE. Therefore, it is crucial to develop more functional coating layers to enhance the performance of sulfide-based AFSSBs. Conversion reaction-based metal compounds, such as metal sulfides, fluorides, and oxides, have emerged as promising candidates for coating layers in LMSSBs and AFSSBs. These compounds undergo conversion reactions during Li plating, dynamically forming Li-metal alloy phases and Li-containing compounds (e.g., Li_2S, LiF).[45,46] The Li-metal alloy promotes uniform Li nucleation and growth, while the Li-containing compounds, which exhibit reasonable ionic conductivity, facilitate Li

https://doi.org/10.1021/acsenergylett.5c00517
ACS Energy Lett. 2025, 10, 2377−2391

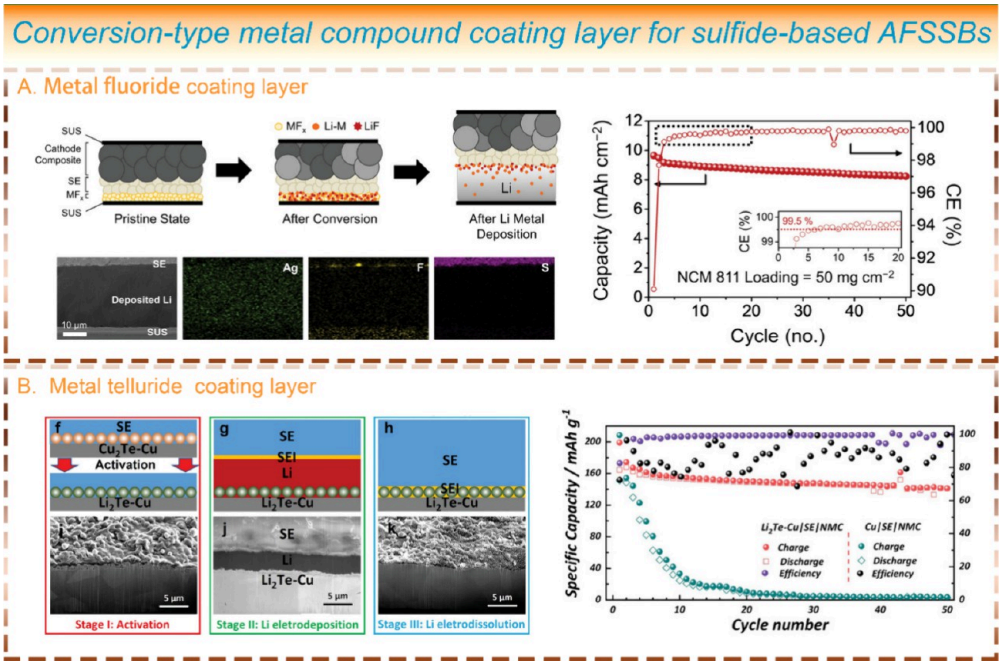

Figure 4. (A) Schematic illustration of Li plating on metal fluoride coating layer. Cycling performance of AgF-based full cell tested at 0.1 C. Reproduced with permission from ref 47. Copyright 2022 Wiley-VCH. (B) Schematic illustration of the evolution of Cu_2Te coating layer during Li deposition and dissolution. The corresponding cross-sectional SEM images were presented at the bottom. Cycling performance comparison of the Cu/SE/NMC and Cu_2Te/SE/NMC cells. Reproduced with permission from ref 48. Copyright 2023 Wiley-VCH.

transfer across the interface and suppress interfacial degradation by preventing direct contact between Li and SE.

For instance, conversion reaction-based metal fluorides have been explored as coating layers to enhance the performance of sulfide-based AFSSBs.[47] Among various metal fluorides, AgF has been identified as a particularly promising candidate due to its ability to support a solid-solution mechanism with a low nucleation overpotential. During the conversion reaction, the formation of Ag nanodomains facilitates an alloy reaction with Li, acting as metal seeds for Li nucleation and promoting uniform Li plating. Simultaneously, LiF, another product of the conversion reaction, prevents the aggregation of Ag nanodomains and mitigates the reduction of sulfide SE, thereby stabilizing the interphase and improving plating/stripping efficiency. As a result, the AgF/SE/NMC full cell achieved a high initial capacity of 9.7 mAh cm^{-2} with a capacity retention of 85.4% after 50 cycles (Figure 4A). Mitlin et al.[48] developed a thin yet uniform $CuTe_2$ coating layer on a Cu CC by simply exposing the Cu substrate to tellurium vapor, enabling high-performance sulfide-based AFSSBs. During the initial charge, $CuTe_2$ undergoes a conversion reaction with Li to form a thin Li_2Te layer, which significantly reduces the Li plating overpotential and improves interfacial stability compared to an unmodified Cu CC. Consequently, the Cu_2Te/SE/NMC full cell exhibited superior cycling stability, with a capacity retention of 80% after 50 cycles, whereas the Cu/SE/NMC full cell experienced rapid capacity degradation, retaining less than 30 mAh g^{-1} after just 10 cycles (Figure 4B).

■ CARBON-BASED INTERLAYER

Although surface modification of the current collector in AFSSBs can promote uniform lithium nucleation and deposition during cycling, it is unable to suppress the undesirable interface side reactions between sulfide SEs and deposited Li, leading to the formation of resistive interphases, such as Li_2S, LiCl, and other degradation products.[12,31,49] In addition, the surface modification layer reacts with Li on charge, forming Li-alloy or Li compounds, which typically undergo considerable volume change. This volume fluctuation can result in aggregation or detachment of the modification layer at the interface during repeated lithium plating/stripping processes. To mitigate the detrimental side reactions, the introduction of an interlayer between the sulfide SE and the current collector has been proposed as a promising strategy.[12,18,19,50,51] The interlayer can, on one hand, physically separate the deposited Li and SE, thus suppressing the undesirable interface side reactions. On the other hand, the interlayer can act as a host to accommodate partial deposited Li and release the mechanical strain at the interface induced by the huge volume change during the repeated plating/stripping. Therefore, the interface contact can be well maintained due to the existence of the interlayer, contributing to the long-term stability of the anode-free batteries. For instance, Lee et al.[19] from Samsung first reported the use of a silver−carbon black (Ag-CB) nanocomposite interlayer in AFSSBs with LPSC as the sulfide electrolyte. The Ag-CB interlayer was prepared by a facile slurry-coating method with a thickness of around 10um, a pouch-type anode-free cell with this Ag-CB interlayer as the anode and a high nickel NMC cathode exhibited a high energy density of over 900 Wh L^{-1} and excellent cycle life exceeding 1000 cycles with an average CE of 99.8% (Figure 5A). The excellent electrochemical performance can be attributed to the two aspects: (1) Ag particles can form Li−Ag alloy on charge and then reduce the Li nucleation energy, thus promoting uniform Li deposition on the current collector; (2) the carbon layer can isolate the SE and deposited Li, avoiding the interfacial side reaction and ensuring good interface contact.

Despite the great success of the Ag-CB interlayer in improving the cycling performance of sulfide-based AFSSBs, several fundamental questions remain unclear. First, the

https://doi.org/10.1021/acsenergylett.5c00517
ACS Energy Lett. 2025, 10, 2377−2391

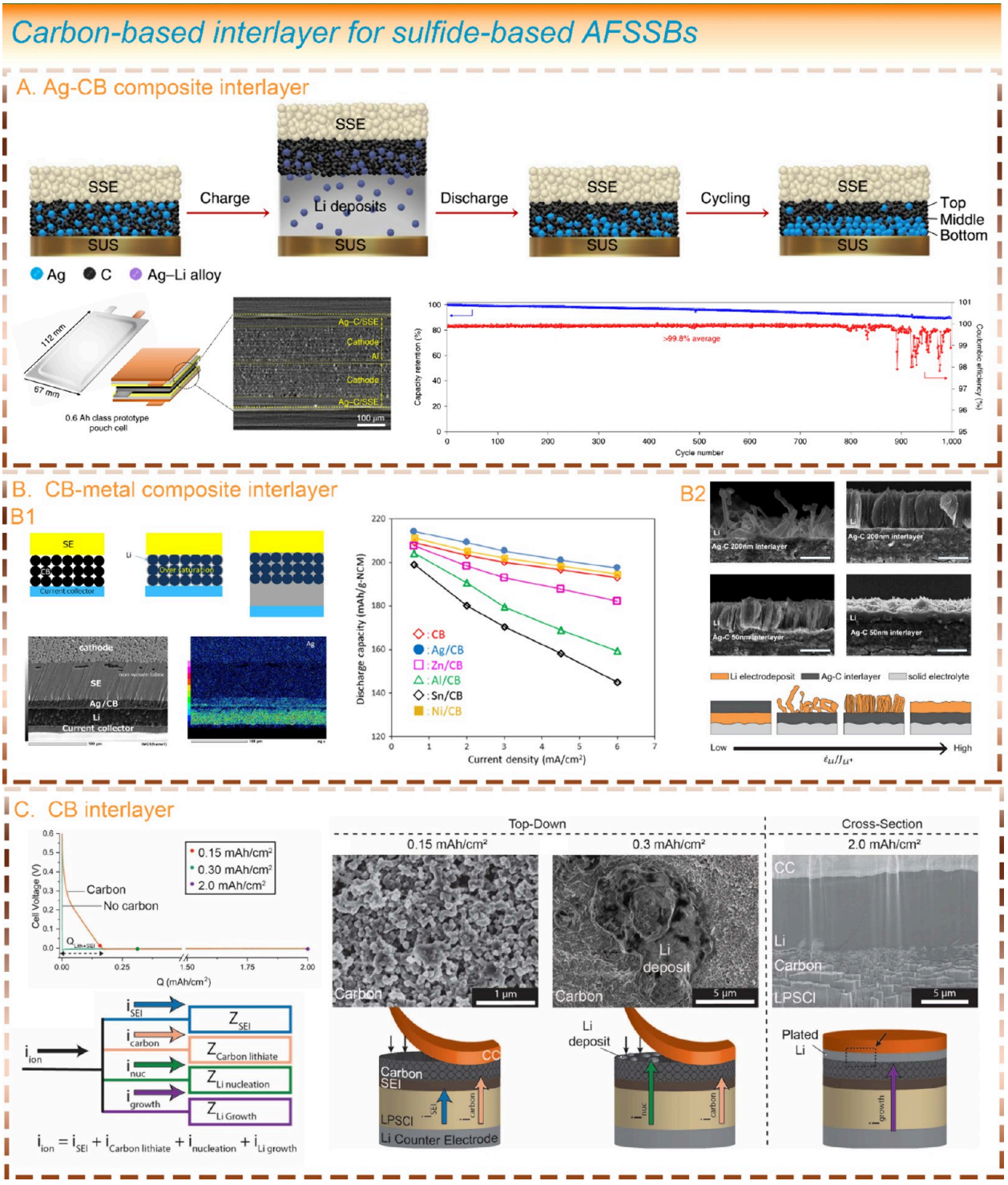

Figure 5. (A) Schematic illustration of Li plating/stripping processes in the anode-free full cell with an Ag−C composite interlayer. Schematic of a 0.6 Ah pouch cell and a bicell structure. Cycling performance of the Ag−C/SE/NMC pouch cell (0.6 Ah) tested at 60 °C. Reproduced with permission from ref 19. Copyright 2020 Springer Nature. (B1) Schematic illustration of CB-based anodes in sulfide-based AFSSBs during charge. Cross-sectional SEM image of the Ag/CB and the corresponding EDX mapping after 1st charge. Rate performance of AFSSBs with different CB-based anodes. Reproduced from ref 52. Available under a CC BY-NC-ND 4.0. Copyright 2021 The Authors. (B2) Cross-sectional SEM images of plated Li under different conditions. Scale bar is 10 μm. Schematic of plated Li morphology varying with J_{Li}^{0}, *creep*/J_{Li}^{+}, *reduction*. Reproduced with permission from ref 53. Copyright 2024 Wiley-VCH. (C) Charge curves of sulfide-based half-cells with/without carbon interlayer at 0.1 mA cm^{-2} with a fixed capacity of 2 mAh cm^{-2}. Schematic illustration of reaction pathways in AFSSBs with a carbon interlayer. Top-down SEM images of the carbon interlayer at different deposition capacities. Cross-sectional SEM image of the carbon interlayer after charging to 2 mAh cm^{-2}. Reproduced from ref 54. Available under a CC-BY 3.0. Copyright 2024 Royal Society of Chemistry.

https://doi.org/10.1021/acsenergylett.5c00517
ACS Energy Lett. 2025, 10, 2377−2391

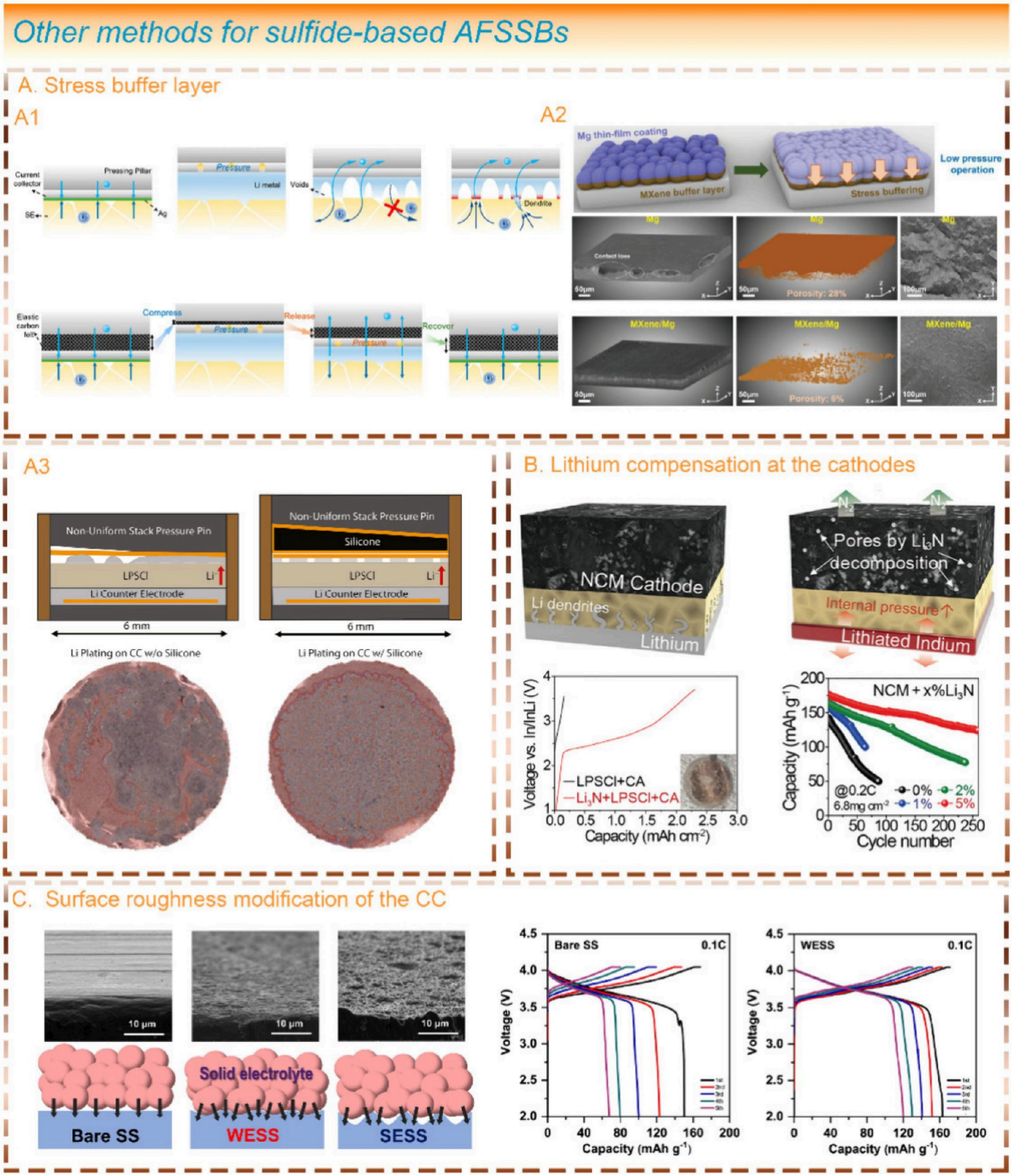

Figure 6. (A1) Schematic illustration of Li plating/stripping processes in AFSSBs with/without carbon felt layer for pressure regulation. Reproduced from ref 55. Available under a CC-BY 4.0. Copyright 2023 American Chemical Society. (A2) Schematic illustration of lithiation with MXene buffer layer. X-ray μ-CT of the anode-SE interfaces of the full cells with/without MXene buffer layer after 10 cycles at a low stack pressure of 2 MPa. Reproduced with permission from ref 56. Copyright 2023 Wiley-VCH. (A3) Li plating with and without a silicone interlayer in sulfide-based AFSSBs. Reproduced with permission from ref 57. Copyright 2025 Elsevier. (B) Schematic illustration of solid-state batteries with/without Li_3N sacrificial cathode during charging process. Voltage profiles show the electrochemical active of Li_3N in solid-state batteries during the first charging. Cycling performance comparison with different contents of Li_3N in the cathode. Reproduced with permission from ref 59. Copyright 2021 Wiley-VCH. (C) Cross-sectional SEM images of the SS foils with under different etching conditions. Schematic of the interface contacts of the SE and the SS with different roughness. Charge−discharge profiles of the AFSSBs with bare SS and weakly etched SS. Reproduced with permission from ref 64. Copyright 2022 Elsevier.

underlying reason for Ag migration to the CC side and its dissolution into plated Li metal upon charge process is unclear. Second, it is unclear why Li only plated at the interlayer-CC interface and what the underlying mechanism is to account for the Li migration within the interlayer. With these questions, Suzuki et al.[52] revisited the CB-M (M = Ni, Zn, Sn, Al, and

https://doi.org/10.1021/acsenergylett.5c00517
ACS Energy Lett. 2025, 10, 2377−2391

Ag) interlayer in sulfide-based AFSSBs (Figure 5B1). In their study, they first examined a pure CB as the interlayer in AFSSBs and found that the cycle stability greatly improved even in the absence of metal particle additives. Additionally, Li layer was observed between the CB interlayer and the CC, suggesting that Li can penetrate the CB interlayer and deposit at the CB-CC interface. Although lacking solid evidence, they provided a speculated explanation on this unnormal Li deposition behavior: the lithiation of carbon took place at the early stage, then the CB layer became oversaturated due to the overpotential, followed by Li deposition in the pores among the CB particles. Finnaly, the pores were filled with Li and the current collector was pushed out by the overflowing Li. A comparison between Ag-CB and other metal-CB revealed that Ag-based interlayer showed superior rate capability and good capacity retention. Cross-sectional SEM and EDX mapping indicated that only Ag migrated to the CB/CC interface while other metals remained within the CB layer, which is because Li has a good solubility in Ag and forms a continuous solid solution with Ag on charge, thereafter the Ag−Li alloy and Li atoms were pushed out and moved together to the current collector by the overflowing Li.

Later, Hatzell et at.[53] further studied the mechanism of Ag−C interlayer in sulfide-based AFSSBs. Their findings corroborated previous observations of Li creeping through the porous interlayer. Moreover, they systematically examined the effects of stack pressure, interlayer composition, and current density on Li migration through the Ag−C interlayer and its influence on Li deposition morphology. Their study culminated in a proposed concept suggesting that the morphology of Li electrodeposits is predominantly governed by the ratio of the Li metal creep flux to the flux of Li accumulation from Li-ion reduction (J_{Li}^{0}, *creep*/J_{Li}^{+}, *reduction*) (Figure 5B2).

Although prior studies proposed a mechanism for the carbon interlayer in sulfide-based AFSSB, which involves the initial lithiation of carbon followed by its oversaturation upon charge, a deep understanding of Li dynamics within the carbon interlayer remains essential and can provide insights on designing promising interlayers for high-performance AFSSBs. Recently, Dasgupta et al.[54] investigated the interfacial dynamic of carbon interlayers in AFSSBs using LPSC SE through a combination of electrochemical analysis and microscopic images (Figure 5C). Their observations aligned with previous studies, revealing initial lithiation of the carbon layer followed by lithium supersaturation and metal deposition. However, they further discovered that the transition between carbon lithiation and Li deposition pathways was closely dependent on the applied current density. Under higher current densities, Li nucleation and deposition commenced before complete lithiation of the carbon interlayer. Moreover, some deposited Li diffused into the incomplete lithiated carbon layer through a solid-state lithiation, leading to gradients of Li concentration within the carbon interlayer. These Li concentration gradients can influence Li nucleation and subsequent solid-state lithiation reactions. This study suggests the complexity of Li dynamics within carbon interlayers upon charge in AFSSBs and provide insights on designing optimal interlayers for high-performance sulfide-based AFSSBs.

OTHER METHODS

In addition to the prevalent strategies mentioned before, alternative approaches have been developed to effectively prolong the cycle life of sulfide-based AFSSBs. As discussed earlier, interfacial contact loss is one of the main factors leading to the poor CE and fast capacity degradation in anode-free solid batteries. To address this issue, our group proposed a self-adjusting interfacial pressure strategy by introducing an elastic carbon felt layer behind the current collector.[55] This elastic layer can greatly release the strain generated from the volume change during Li plating and stripping, ensuring intimate interfacial contact at the end of fully stripping (Figure 6A1). Consequently, the AFSSBs with the carbon felt layer exhibited an increased initial CE from 58.4% to 83.7% as well as enhanced cyclic stability. Later, Choi et al.[56] developed a different approach by incorporating a ductile Ti_3C_2Tx MXene buffer layer beneath a Mg thin film at the anode (Figure 6A2). This configuration enabled the practical operation of sulfide-based AFSSBs at room temperature under a low pressure of 2 MPa. Using microcomputed tomography (μ-CT), they observed a smoother interface between the anode and solid electrolyte in the cycled MXene/Mg electrode, whereas severe interfacial contact loss was detected in the cycled Mg-only electrode. Additionally, the MXene/Mg electrode exhibited a lower internal porosity of 6%, compared to 28% in the Mg-only electrode. The ductile nature of the MXene layer was crucial in buffering volume changes and alleviating mechanical stress during lithium plating and stripping. More recently, Dasgupta et al.[57] introduced a thin elastomeric silicone interlayer behind the CC to promote uniform stress distribution, leading to a significant improvement in Li plating areal coverage (Figure 6A3). As a result, the first-cycle CE increased from 89% to 94% due to the more uniform pressure distribution.

Another promising strategy for enhancing the cycle life of anode-free batteries is lithium compensation strategy at the cathodes. In anode-free batteries, the Li-containing cathodes are the sole source of Li ions for cycling. However, anode-free batteries often experience unavoidable irreversible capacity loss during the initial cycle. To address this, enhancing lithium inventory at the cathodes can compensate for the loss of active Li ions in the first cycle and provide an additional lithium reservoir for subsequent cycles. There are generally two prevalent methods for enhancing lithium inventory at the cathodes. One method involves incorporating a Li-containing compound, such as Li_2O,[58] Li_3N,[59] or Li_2S,[60] into the cathode composites. These compounds release Li ions during the charging process through an oxidation reaction. Another approach is to chemically or electrochemically preinsert Li into the Li-containing cathodes, such as NMC811 or manganese-based spinel cathodes.[61,62] Both methods have been demonstrated to be highly effective in liquid-based anode-free lithium−metal batteries. However, lithium compensation strategy at the cathodes in sulfide-based all-solid-state batteries (AFSSBs) remains in its early stages, with limited research available. This is due to the additional challenges faced by solid-state anode-free batteries compared to their liquid-based counterparts. In 2022, B. Kim et al.[59] studied the effect of a Li_3N sacrificial cathode additive on the cycling performance of sulfide-based Li-free SSBs coupled with an In anode (Figure 6B). The oxidation decomposed Li_3N provided extra Li to offset the active Li loss due to the side reaction. Meanwhile, the additional Li increased the volume expansion of the In layer, leading to an enhanced internal cell pressure and good physical contact at the anode/SE interface. As a result, the cell with 5% Li_3N exhibited significantly enhanced cycling performance. However, since the study employed an In anode, it was not a true anode-free system.

https://doi.org/10.1021/acsenergylett.5c00517
ACS Energy Lett. 2025, 10, 2377−2391

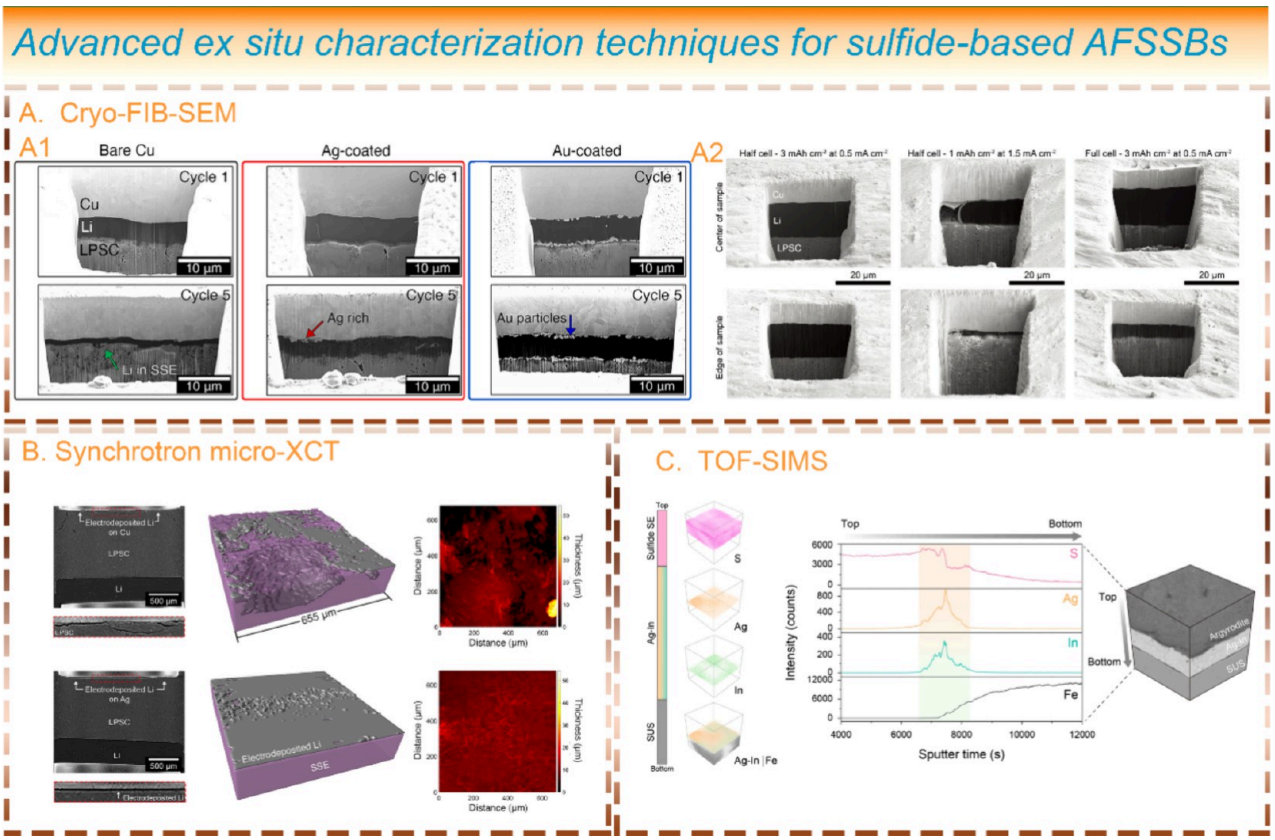

Figure 7. (A1) Cryo-FIB-SEM images of Li deposited on bare Cu, Ag-coated Cu, Au-coated Cu after the 1st and 5th cycles. Reproduced with permission from ref 65. Copyright 2023 Elsevier. (A2) Cryo-FIB-SEM images of the Cu-SE interfaces after Li deposition under different cycling conditions. Reproduced with permission from ref 66. Copyright 2023 Wiley-VCH. (B) Synchrotron micro-XCT of the bare Cu and Ag-coated Cu after deposition of 2 mAh cm^{-2} Li at 0.5 mAh cm^{-2}. Reproduced with permission from ref 65. Copyright 2023 Elsevier. (C) TOF-SIMS 3D images of the SE, In-doped Ag coating layer, and SS, and the corresponding depth profiles of elements S, Ag, In, and Fe. Reproduced with permission from ref 41. Copyright 2024 Elsevier.

Later, Lee et al.[40] reported a sulfide-based AFSSBs with excellent capacity retention of 80% over 500 cycles through a combination of Mg layer at the anode side and Li_3N additive at the cathode side. These studies highlight the potential of lithium compensation strategy at the cathodes in improving AFSSB performance when combined with other mechanical and chemical strategies.

Previous research has shown that surface modification of the current collector (CC) via the deposition of a thin nanolayer can significantly enhance the cycle performance of sulfide-based AFSSBs. However, the addition of extra layers compromises some advantages of AFSSBs, such as cost-efficiency, simplified design, and high energy density. An alternative approach is to modify the surface roughness of the CC without introducing additional materials. By adjusting the microscopic surface structure, charge accumulation sites can be tailored, reducing local current density and enabling more uniform interfacial contact. For instance, Eom et al.[63] used a pulse-reverse polarization method to control the surface roughness of the metal CC, studying its effects on the stability of anode-free lithium−metal batteries (AFLMBs) in liquid electrolytes. They found that Li deposited on the roughened CC had a denser and flatter morphology compared to the needle-like dendrites observed on untreated CCs. The impact of CC surface roughness on the reversibility of Li plating and stripping in sulfide-based AFSSBs has also been investigated. Park et al.[64] created surface-roughened stainless-steel CCs with varying roughness using a simple acid etching method and examined the correlation between surface roughness and cycle stability in AFSSBs (Figure 6C). Their results indicated that moderately roughened CCs provided more interfacial contact points, allowing for more uniform lithium deposition. In contrast, both bare and excessively roughened CCs deteriorated cycling performance due to limited contact points. These findings offer valuable insights into designing advanced CCs for high-performance AFSSBs.

■ ADVANCED CHARACTERIZATION TOOLS FOR SULFIDE-BASED AFSSBS

In the previous sections, we have comprehensively summarized strategies for improving the cyclic life of sulfide-based AFSSBs. However, the fundamental mechanisms governing the effectiveness of these strategies, as well as the associated failure processes, remain insufficiently understood. Gaining deeper insight into these mechanisms is crucial for advancing the development of sulfide-based AFSSBs and optimizing their long-term performance. To address this knowledge gap, it is imperative to employ advanced characterization techniques—such as ex-situ, in situ, and operando methods—that enable the diagnosis of failure mechanisms and provide a deeper understanding of the working principles of strategies designed to prolong battery lifespan.

https://doi.org/10.1021/acsenergylett.5c00517
ACS Energy Lett. 2025, 10, 2377−2391

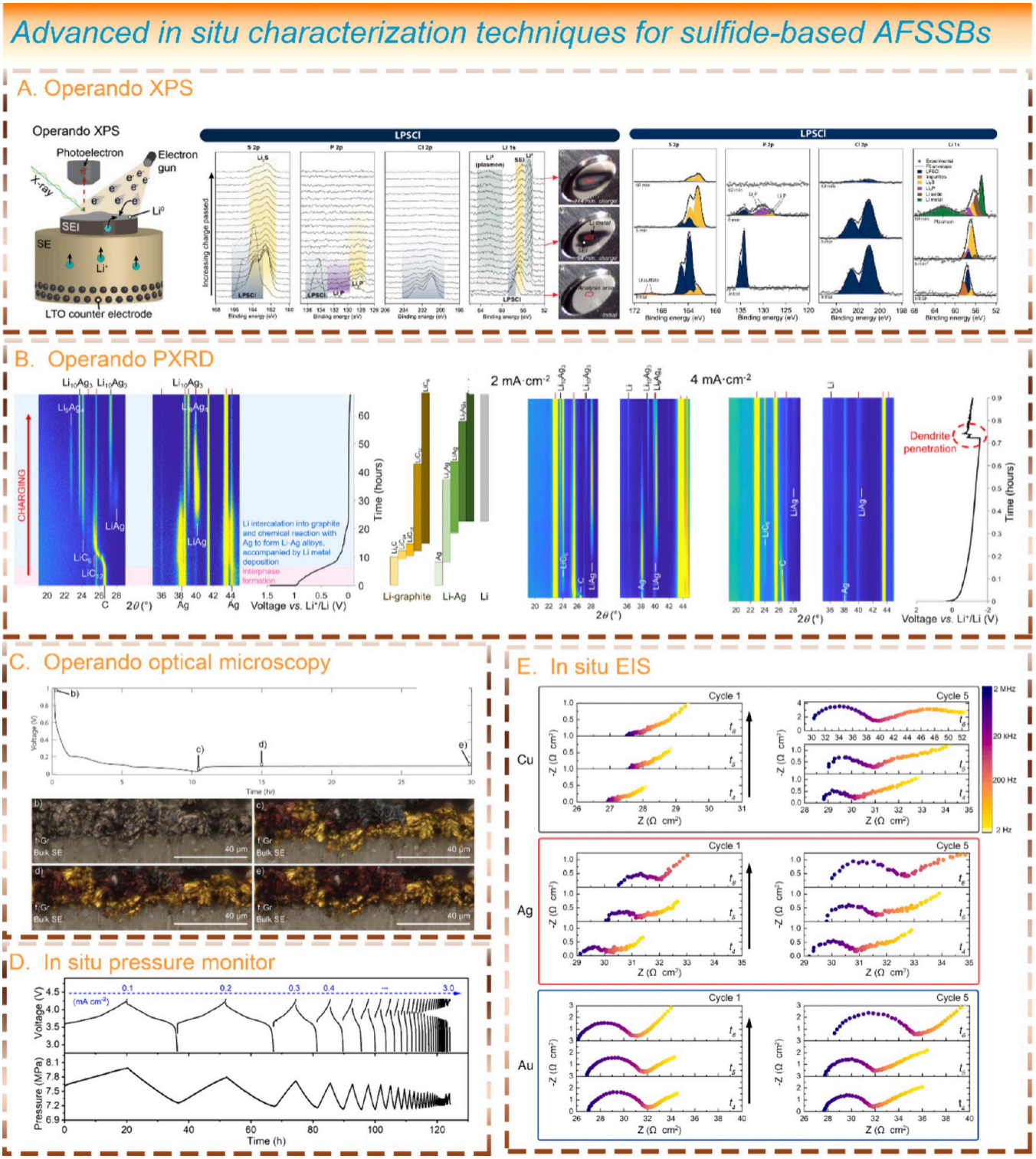

Figure 8. (A) Schematic of operando XPS anode-free solid-state cell with an electron gun as a virtual electrode. Operando XPS core scans and the corresponding optical images of anode-free surface throughout the experiment. Operando XPS spectra of S 2p, P 2p, Cl 2p, and Li 1s peak fits. Reproduced with permission from ref 67. Copyright 2021 IOPscience. (B) Operando PXRD patterns of the Ag-G interlayer at the anode of an LPSC-based anode-free cell during charge at 30 μA cm^{-2}. Operando PXRD patterns of the Ag-G interlayer at the anode of an LPSC-based anode-free cell during charge at higher current densities of 2 mA cm^{-2} and 4 mA cm^{-2}. Reproduced from ref 68. Available under a CC-BY 4.0. Copyright 2023 The Authors. (C) Operando optical microscopy images of the graphite interlayer under different electrochemical states: before cycle, after lithiation, after 5 h OCV rest, and after 20 h OCV rest. Reproduced from ref 54. Available under a CC-BY 3.0. Copyright 2024 Royal Society of Chemistry. (D) CCD measurement of the carbon felt-based AFSSBs and the corresponding in situ stack pressure monitoring during the CCD measurement. Reproduced with permission from ref 55. Copyright 2023 American Chemical Society. (E) In-situ EIS measurements of the bare Cu half-cell, Ag-coated Cu half-cell, and Au-coated Cu half-cell at times t4 to t6 during Li stripping at the 1st cycle and 5th cycle. Reproduced with permission from ref 65. Copyright 2023 Elsevier.

https://doi.org/10.1021/acsenergylett.5c00517
ACS Energy Lett. 2025, 10, 2377−2391

EX SITU CHARACTERIZATION TECHNIQUES

Characterizing the deposited Li/SE interface is crucial in AFSSBs since interfacial properties significantly influence cycling stability. A poorly formed Li/SE interface can lead to rapid capacity decay. However, interface characterization in AFSSBs presents significant challenges due to several factors: (1) the interfaces are buried within the SE and CC, complicating direct observation and characterization with conventional surface analysis techniques; and (2) the highly reactive nature of deposited Li makes preserving the pristine state of the interfaces during sample preparation and characterization particularly challenging.

To address these challenges, cryo-focused ion beam (FIB) milling coupled with cross-sectional SEM has been employed. Cryo-FIB operates at cryogenic temperatures, preserving the native state of deposited Li and preventing damage to the interfaces. For example, McDowell et al.[65] utilized cryo-FIB-SEM to investigate the influence of alloy interfacial layers on the interfacial morphology evolution in sulfide-based AFSSBs. They compared cryo-FIB-SEM images of Li plated on different substrates (bare Cu, Ag-coated Cu, and Au-coated Cu), demonstrating that the cryogenic environment during sample milling preserved the native state of deposited Li (Figure 7A1). The thickness of deposited Li across the three cells was approximately 5 μm after one cycle, consistent with the theoretical thickness of 1 mAh cm^{-2} of Li. However, after five cycles, the Li on bare Cu was thin and nonuniform, with substantial Li growth within the SE. In contrast, the Li on Ag-coated Cu was thicker and more uniform, though aggregation of Ag particles at the Li/Cu interface was observed, potentially affecting long-term cycling performance. Similarly, Li deposition on Au-coated Cu was more uniform than on Ag-coated Cu. Cryo-FIB-SEM thus provides direct evidence that alloy interfacial layers can effectively promote uniform Li deposition in AFSSBs. Additionally, cryo-FIB-SEM has been employed to study short-circuit-induced failures in AFSSBs by examining the evolution of the thickness and structure of deposited Li at various interface positions (Figure 7A2). Lewis and co-workers[66] observed uniform Li thickness across the interface at a low deposition current density of 0.5 mA cm^{-2} in a Cu/LPSC/Li half-cell. However, at a higher current density of 1.5 mA cm^{-2}, the Li thickness became nonuniform, with significantly thinner deposition at the electrode edges. Interestingly, in a Cu/LPSC/NMC full cell, Li thickness was lower at the electrode edges and higher at the center, despite plating the same areal capacity at the same current density of 0.5 mA cm^{-2}. The reasons for this nonuniform Li deposition in full cells remain unclear.

Although cryo-FIB-SEM is a powerful technique for studying the anode interface morphology and structure in AFSSBs, its application is typically constrained to micrometer-scale regions, limiting its ability to capture macroscopic features or larger sample heterogeneities. To address this limitation, synchrotron X-ray computed tomography (micro-XCT) has been proposed as an alternative, enabling the characterization of much larger regions (millimeter to centimeter scale) and capturing the overall 3D architecture of larger samples. For instance, McDowell et al.[65] utilized synchrotron micro-XCT to study the deposited Li (2 mAh cm^{-2}) on bare Cu and Ag-coated Cu electrodes in half-cells (Figure 7B). The micro-XCT results revealed that Li on bare Cu grows nonuniformly with varying thickness across the interface, whereas Li on Ag-coated Cu exhibits uniform deposition. Additionally, 3D renderings of the Li/SE phases showed that Li on Cu displayed nonuniform coverage of the interface and significant Li growth within the SE, while Li on Ag-coated Cu demonstrated uniform coverage and no observable Li growth within the SE. These findings align with their previously discussed cryo-FIB-SEM results, further validating the advantages of alloy-coated current collectors in promoting uniform Li deposition.

While cryo-FIB-SEM and synchrotron micro-XCT are powerful tools for analyzing the interface morphologies of AFSSBs, it is equally important to investigate interface chemistry and diagnose degradation mechanisms. Time-of-Flight Secondary Ion Mass Spectrometry (TOF-SIMS) offers unique capabilities, including depth profiling, high elemental sensitivity, and spatial resolution, making it particularly well-suited for studying interface chemistry in sulfide-based AFSSBs. For instance, Yu et al.[41] employed TOF-SIMS depth profiling to visualize the distribution of In and Ag in the In-doped Ag coating layer on SS for sulfide-based AFSSBs (Figure 7C). The results revealed that a small amount of In is uniformly distributed within the In−Ag layer, indicating that In is soluble in the Ag crystal lattice.

IN SITU/OPERANDO CHARACTERIZATION TECHNIQUES

Advanced ex-situ characterization techniques, such as cryo-FIB-SEM, are effective in investigating the morphological and structural evolution of the Li/SE interface in AFSSBs. However, developing in situ/operando characterization techniques is essential for unveiling the complex interplay of chemical, mechanical, and electrochemical processes in AFSSBs, providing profound insights into the underlying mechanisms and enabling the design of promising strategies to enhance long-term cycling performance. In situ/operando techniques facilitate real-time monitoring of Li nucleation, plating, and stripping processes, offering insights into time-dependent phenomena inaccessible with ex-situ methods. Furthermore, these techniques enable real-time tracking of Li/SE interface dynamics under operational conditions, providing insights into the formation and evolution of the solid electrolyte interphase (SEI) and unraveling degradation mechanisms. Nevertheless, designing feasible in situ/operando techniques for sulfide-based AFSSBs presents significant challenges compared to liquid-based batteries.

Davis et al.[67] developed an operando X-ray photoelectron spectroscopy (XPS) technique to study the chemical evolution of the anode-free surface during SEI formation and initial Li nucleation in a sulfide-based AFSSB (Figure 8A). The operando XPS cell was constructed with an LTO counter electrode and LPSC as the SE, where the electron gun acted as a virtual electrode, providing electron flux to the SE surface. A potential gradient forms when charges accumulate at the SE surface, driving Li^+ migration from LTO to the LPSC surface, where Li^+ reacts with electrons and a reduction reaction occurs. The evolution of S, P, and Cl XPS spectra suggests that the SEI forms prior to Li nucleation. The evolution of Li XPS spectra reveals that the main reaction pathway shifted to Li metal nucleation and growth once the SEI became sufficiently thick to impede electron transfer to the SEI/SE interface. Operando XPS enables dynamic investigation of the evolution of interface chemistries in AFSSBs and provides insights into the causes of low efficiency and capacity loss.

https://doi.org/10.1021/acsenergylett.5c00517
ACS Energy Lett. 2025, 10, 2377−2391

In previous discussions, the interlayer strategy has demonstrated significant success in enhancing the cycling performance of AFSSBs, particularly the carbon-Ag nanocomposite interlayer, which can stabilize cycling performance for over 1000 cycles. However, the structural evolution of the interlayer during cycling remains unclear, underscoring the importance of investigating its functional mechanisms. To address this, Bruce et al.[68] designed operando powder X-ray diffraction (PXRD) to dynamically monitor the structural evolution of an Ag-graphite (Ag-G) composite interlayer during Li plating/stripping in LPCS-based AFSSBs. Operando PXRD revealed that Li initially intercalates chemically into graphite, and the lithiated graphite reacts with Ag to form a series of increasingly Li-rich LiAg alloys, with simultaneous Li metal plating (Figure 8B). Interestingly, operando PXRD indicated that the lithiation of graphite occurs more rapidly than the chemical reaction with Ag, leading to the formation of Li-deficient LiAg alloys until a higher state of charge at a higher charge current density, which is less effective in suppressing Li dendrites. Consequently, identifying carbon materials with high Li diffusivity is crucial for mitigating Li dendrite formation in AFSSBs under practical conditions.

In Section 4.1, we discussed the critical role of cryo-FIB-SEM in analyzing the morphologies of deposited Li in AFSSBs. However, these techniques can only capture Li morphology at specific charge or discharge states, lacking the capability to monitor morphology evolution in real time. Operando optical microscopy is a crucial technique that facilitates direct, real-time visualization of Li deposition and stripping processes in AFSSBs, allowing dynamic monitoring of morphological changes at the anode interface. Liao et al.[54] performed operando video microscopy to investigate the interfacial dynamics of a carbon interlayer during the lithiation process in sulfide-based AFSSBs. Graphite was selected as the carbon interlayer because its color changes as a function of the degree of lithiation, enhancing interlayer visualization. Operando optical microscopy revealed a lithium concentration gradient within the carbon interlayer during the initial charge (Figure 8C). This gradient relaxes during the OCV rest through a solid-state diffusion mechanism. At higher charge rates, the Li concentration gradient increases, leading to Li metal deposition before the incomplete lithiation of graphite.

In AFSSBs, stack pressure is a key parameter influencing cycling performance. Insufficient pressure can result in poor contact at the anode/SE interface, leading to high interfacial resistance and sluggish Li^+ transport. Conversely, excessive stack pressure may cause electrochemically plated Li to creep into pores or voids within the SE layer, potentially inducing soft shorts. Therefore, optimizing stack pressure is essential for maintaining stable interface contact and prolonging the cycle life of AFSSBs. For example, Han et al.[69] proposed a Li-metal-compatible hydride-based interlayer (LBHI) to suppress side reactions between plated Li and LPSC. While the interlayer effectively stabilized the interface in a Cu/LBHI/LPSC/Li−In half-cell, achieving an improved initial CE of 94.7%, the Cu/LBHI/LPSC/NCA full cell exhibited poor stability, with a soft short occurring after the 10th cycle. They observed a drop in stack pressure from 15 MPa initially to approximately 0.4 MPa after 10 cycles, underscoring the critical importance of stable stack pressure in AFSSBs. Our group proposed the use of an elastic carbon felt to regulate pressure during Li plating/stripping.[55] An in situ pressure monitoring technique was utilized to elucidate the role of the elastic carbon felt in stabilizing sulfide-based AFSSBs. Real-time pressure tracking curves revealed minimal pressure changes during the critical current density (CCD) measurements of AFSSBs (Figure 8D). These findings further highlight the significance of stack pressure in achieving stable and reliable AFSSB performance.

In addition to the aforementioned operando techniques, operando electrochemical impedance spectroscopy (EIS) is another accessible yet essential method capable of capturing the real-time evolution of interfacial resistance during Li plating/stripping processes, providing critical insights into the mechanisms underlying capacity degradation. For example, McDowell et al.[65] utilized operando EIS spectra to examine the interfacial resistance evolution in three anode-free solid half-cells employing Cu, Ag-coated Cu, and Au-coated Cu as anode current collectors (Figure 8E). Operando EIS spectra indicated that the Cu cell exhibited minimal interfacial resistance variation during the first stripping process; however, it showed a significant increase in interfacial resistance at the beginning of the fifth stripping, which further escalated near the end of the fifth stripping (t6). Additionally, a pronounced semicircle emerged in the low-frequency region during the fifth stripping process, attributed to interface contact loss caused by deep stripping. In contrast, the Ag-coated cell displayed a minimal semicircle, while the Au-coated cell exhibited no semicircle in the low-frequency region near the end of the fifth stripping process (t6). These results suggest that Ag and Au-seeded current collectors can effectively mitigate void formation and interface contact loss, thereby enhancing the performance of AFSSBs.

SUMMARIES AND PERSPECTIVES

Sulfide-based AFSSBs represent a promising class of next-generation energy storage devices, offering advantages of high energy density, enhanced safety, and simplified manufacturing processes. However, their practical implementation is hindered by three critical challenges: nonuniform Li nucleation leading to dendrite formation, unstable interfaces between plated Li and sulfide SEs causing resistance buildup, and interfacial void formation resulting in capacity decay. To address these issues, several effective strategies have been developed, including metal seed coatings (e.g., Ag, Mg) for uniform lithium deposition, carbon-based interlayers (notably the Samsung-developed silver−carbon composite achieving 1000+ cycles) for interface stabilization, and various supplementary approaches such as pressure regulation, cathode prelithiation, and surface roughening of current collectors. Understanding these challenges and validating solutions has been greatly facilitated by advanced characterization techniques, including cryo-FIB-SEM, synchrotron X-ray tomography, and in situ/operando methods, which provide crucial insights into failure mechanisms and interface evolution during battery operation.

Despite the promising advancements in sulfide-based AFSSBs, the field remains in its early stages, and numerous challenges persist. To advance the development of sulfide-based AFSSBs and accelerate their commercialization, more endeavors are needed to fundamentally understand the underlying scientific issues causing the rapid capacity decay and to explore potential strategies for improving the room temperature long-term cycle stability with average CE approximately 99.9%. Therefore, we propose future perspectives to advance this innovative technology.

Advanced Characterization Techniques. Understanding the working and failure mechanisms of sulfide-based

https://doi.org/10.1021/acsenergylett.5c00517
ACS Energy Lett. 2025, 10, 2377−2391

AFSSBs requires sophisticated in situ/operando image characterization techniques to real-time track the Li nucleation and growth process. For instance, in situ cryo-electron microscopy (cryo-EM) is a powerful tool to monitor Li nucleation and subsequent growth at nano/atomic scale. Additionally, operando synchrotron neutron image and X-ray tomography can provide critical insights into interfacial evolution and failure mechanisms of sulfide-based AFSSB-s.Understanding the working and failure mechanisms of sulfide-based AFSSBs requires sophisticated operando characterization techniques to real-time track the Li nucleation and growth process at the anode interface during initial cyclings.

> Understanding the working and failure mechanisms of sulfide-based AFSSBs requires sophisticated operando characterization techniques to real-time track the Li nucleation and growth process at the anode interface during initial cyclings.

Current Collector Engineering. Commercial bare CCs often lead to nonuniform Li nucleation and deposition. Modifying the CC with lithophilic coating layers is crucial. Ag seed has been proven to be effective in promoting uniform Li nucleation and growth in AFSSBs. However, the use of noble Ag metal undoubtedly increases the manufacturing costs of the cell. Therefore, exploring non-noble metals, such as Zn, Al, and Sn, or metal alloys with minor Ag doping may offer a cost-effective alternative. Additionally, developing lightweight composite current collectors can further improve the energy density of the AFSSBs.

Interlayer Engineering. Although carbon-based interlayers can suppress the interfacial reactions between the plated Li and sulfide SEs, the ionic conductivity of carbon at room temperature is low, which limits the room temperature cycling performance. Developing thin and stable interlayers with high room temperature ionic conductivity is necessary to enable room temperature high-performance sulfide-based AFSSBs.

> Developing thin and stable interlayers with high room temperature ionic conductivity is necessary to enable room temperature high-performance sulfide-based AFSSBs.

Lithium Compensation at the Cathodes. The loss of active Li during the initial charge is a major issue in sulfide-based AFSSBs. Thus, it is essential to compensate for the active Li loss. By adding Li-containing salts or Li-rich cathode in the cathode composites could be a complementary of the limited active Li from the cathode, thus improving the cycle stability of the sulfide-based AFSSBs.

Advanced Manufacturing Techniques. The commercialization of sulfide-based AFSSBs requires the development of advanced dry-processing methods for fabricating thin-film sulfide SEs and cathode electrodes with high tap density. Moreover, reducing stack pressure while maintaining effective electrode−electrolyte contact is crucial. For example, warm-isostatic-pressure has shown promise in densifying the AFSSBs and ensuring a good interface contact at low stack pressures.

These future directions will be instrumental in overcoming the current limitations of sulfide-based AFSSBs and advancing their commercial viability.

AUTHOR INFORMATION

Corresponding Author

Hongli Zhu − *Department of Mechanical and Industrial Engineering, Northeastern University, Boston, Massachusetts 02115, United States;* orcid.org/0000-0003-1733-4333; Email: h.zhu@neu.edu

Author

Jiwei Wang − *Department of Mechanical and Industrial Engineering, Northeastern University, Boston, Massachusetts 02115, United States*

Complete contact information is available at: https://pubs.acs.org/10.1021/acsenergylett.5c00517

Notes

The authors declare no competing financial interest.

Biographies

Dr. Jiwei Wang received his Ph.D. (2020) degree in Chemistry from the University of Western Ontario. He is currently a postdoctoral research associate in Mechanical and Industrial Engineering at Northeastern University. His current research is focused on sulfide-based anode-free solid-state batteries.

Dr. Hongli Zhu is an associate professor at Northeastern University (https://coe.northeastern.edu/research/hongli_group/), directing the Advanced and Intelligent Manufacturing program. Her research spans electrochemical energy storage, sustainable biomass materials, and advanced manufacturing. With over 22,000 citations (H-index: 73), she's recognized among Stanford's Top 2% Scientists Worldwide and has received multiple prestigious awards.

ACKNOWLEDGMENTS

H.Z. acknowledges financial support from the Office of Science Department of Energy under Award Number DESC0024528.

REFERENCES

(1) Sarmah, S.; Lakhanlal; Kakati, B. K.; Deka, D. Recent advancement in rechargeable battery technologies. *WIREs Energy and Environment* **2023**, *12* (2), No. e461.

(2) Choi, J. U.; Voronina, N.; Sun, Y. K.; Myung, S. T. Recent Progress and Perspective of Advanced High-Energy Co-Less Ni-Rich Cathodes for Li-Ion Batteries: Yesterday, Today, and Tomorrow. *Adv. Energy Mater.* **2020**, *10* (42), 2002027.

(3) Dunn, B.; Kamath, H.; Tarascon, J.-M. Electrical Energy Storage for the Grid: A Battery of Choices. *Science* **2011**, *334* (6058), 928−935.

(4) Etacheri, V.; Marom, R.; Elazari, R.; Salitra, G.; Aurbach, D. Challenges in the development of advanced Li-ion batteries: a review. *Energy Environ. Sci.* **2011**, *4* (9), 3243.

(5) Louli, A. J.; Eldesoky, A.; Weber, R.; Genovese, M.; Coon, M.; deGooyer, J.; Deng, Z.; White, R. T.; Lee, J.; Rodgers, T.; Petibon, R.; Hy, S.; Cheng, S. J. H.; Dahn, J. R. Diagnosing and correcting anode-free cell failure via electrolyte and morphological analysis. *Nature Energy* **2020**, *5* (9), 693−702.

(6) Lai, X.; Chen, Q.; Tang, X.; Zhou, Y.; Gao, F.; Guo, Y.; Bhagat, R.; Zheng, Y. Critical review of life cycle assessment of lithium-ion batteries for electric vehicles: A lifespan perspective. *eTransportation* **2022**, *12*, 100169.

(7) Lin, D.; Liu, Y.; Cui, Y. Reviving the lithium metal anode for high-energy batteries. *Nat. Nanotechnol.* **2017**, *12* (3), 194−206.
(8) Xu, W.; Wang, J.; Ding, F.; Chen, X.; Nasybulin, E.; Zhang, Y.; Zhang, J.-G. Lithium metal anodes for rechargeable batteries. *Energy Environ. Sci.* **2014**, *7* (2), 513−537.
(9) Xia, S.; Wu, X.; Zhang, Z.; Cui, Y.; Liu, W. Practical Challenges and Future Perspectives of All-Solid-State Lithium-Metal Batteries. *Chem.* **2019**, *5* (4), 753−785.
(10) Kato, Y.; Hori, S.; Kanno, R. Li10GeP2S12-Type Superionic Conductors: Synthesis, Structure, and Ionic Transportation. *Adv. Energy Mater.* **2020**, *10* (42), 2002153.
(11) Zhang, Q.; Cao, D.; Ma, Y.; Natan, A.; Aurora, P.; Zhu, H. Sulfide-Based Solid-State Electrolytes: Synthesis, Stability, and Potential for All-Solid-State Batteries. *Adv. Mater.* **2019**, *31*, No. e1901131.
(12) Wang, C.; Adair, K. R.; Liang, J.; Li, X.; Sun, Y.; Li, X.; Wang, J.; Sun, Q.; Zhao, F.; Lin, X.; Li, R.; Huang, H.; Zhang, L.; Yang, R.; Lu, S.; Sun, X. Solid-State Plastic Crystal Electrolytes: Effective Protection Interlayers for Sulfide-Based All-Solid-State Lithium Metal Batteries. *Adv. Funct. Mater.* **2019**, *29*, 1900392.
(13) Cao, D.; Sun, X.; Li, Q.; Natan, A.; Xiang, P.; Zhu, H. Lithium Dendrite in All-Solid-State Batteries: Growth Mechanisms, Suppression Strategies, and Characterizations. *Matter* **2020**, *3* (1), 57−94.
(14) Burton, M.; Narayanan, S.; Jagger, B.; Olbrich, L. F.; Dhir, S.; Shibata, M.; Lain, M. J.; Astbury, R.; Butcher, N.; Copley, M.; Kotaka, T.; Aihara, Y.; Pasta, M. Techno-economic assessment of thin lithium metal anodes for solid-state batteries. *Nature Energy* **2025**, *10*, 135−147.
(15) Wang, M. J.; Carmona, E.; Gupta, A.; Albertus, P.; Sakamoto, J. Enabling ″lithium-free″ manufacturing of pure lithium metal solid-state batteries through in situ plating. *Nat. Commun.* **2020**, *11* (1), 5201.
(16) Huang, W. Z.; Zhao, C. Z.; Wu, P.; Yuan, H.; Feng, W. E.; Liu, Z. Y.; Lu, Y.; Sun, S.; Fu, Z. H.; Hu, J. K.; Yang, S. J.; Huang, J. Q.; Zhang, Q. Anode-Free Solid-State Lithium Batteries: A Review. *Adv. Energy Mater.* **2022**, *12* (26), 2201044.
(17) Wen, J.; Wang, T.; Wang, C.; Dai, Y.; Song, Z.; Liu, X.; Yu, Q.; Zheng, X.; Ma, J.; Luo, W.; Huang, Y. A Tailored Interface Design for Anode-Free Solid-State Batteries. *Adv. Mater.* **2024**, *36* (6), No. e2307732.
(18) Kim, K. H.; Lee, M. J.; Ryu, M.; Liu, T. K.; Lee, J. H.; Jung, C.; Kim, J. S.; Park, J. H. Near-strain-free anode architecture enabled by interfacial diffusion creep for initial-anode-free quasi-solid-state batteries. *Nat. Commun.* **2024**, *15* (1), 3586.
(19) Lee, Y.-G.; Fujiki, S.; Jung, C.; Suzuki, N.; Yashiro, N.; Omoda, R.; Ko, D.-S.; Shiratsuchi, T.; Sugimoto, T.; Ryu, S.; Ku, J. H.; Watanabe, T.; Park, Y.; Aihara, Y.; Im, D.; Han, I. T. High-energy long-cycling all-solid-state lithium metal batteries enabled by silver-carbon composite anodes. *Nature Energy* **2020**, *5* (4), 299−308.
(20) Kim, J.; Lee, S.; Kim, J.; Park, J.; Lee, H.; Kwon, J.; Sun, S.; Choi, J.; Paik, U.; Song, T. Regulating Li electrodeposition by constructing Cu-Sn nanotube thin layer for reliable and robust anode-free all-solid-state batteries. *Carbon Energy* **2024**, *6*, No. e610.
(21) Temesgen, N. T.; Bezabh, H. K.; Weret, M. A.; Shitaw, K. N.; Nikodimos, Y.; Taklu, B. W.; Lakshmanan, K.; Yang, S.-C.; Jiang, S.-K.; Huang, C.-J.; Wu, S.-H.; Su, W.-N.; Hwang, B. J. Solvent-free design of argyrodite sulfide composite solid electrolyte with superb interface and moisture stability in anode-free lithium metal batteries. *J. Power Sources* **2023**, *556*, 232462.
(22) Xu, X.; Chu, S.; Xu, S.; Li, H.; Sheng, C.; Dong, M.; Guo, S.; Zhou, H. Integrating Prelithiation and Interface Protection to Achieve High-Energy All-Solid-State Batteries. *Angew. Chem.* **2025**, *64*, No. e202415891.
(23) Sandoval, S. E.; Haslam, C. G.; Vishnugopi, B. S.; Liao, D. W.; Yoon, J. S.; Park, S. H.; Wang, Y.; Mitlin, D.; Hatzell, K. B.; Siegel, D. J.; Mukherjee, P. P.; Dasgupta, N. P.; Sakamoto, J.; McDowell, M. T. Electro-chemo-mechanics of anode-free solid-state batteries. *Nat. Mater.* **2025**, *62*, 9370.
(24) Molaiyan, P.; Abdollahifar, M.; Boz, B.; Beutl, A.; Krammer, M.; Zhang, N.; Tron, A.; Romio, M.; Ricci, M.; Adelung, R.; Kwade, A.; Lassi, U.; Paolella, A. Optimizing Current Collector Interfaces for Efficient "Anode-Free" Lithium Metal Batteries. *Adv. Funct. Mater.* **2024**, *34* (6), 2311301.
(25) Pande, V.; Viswanathan, V. Computational Screening of Current Collectors for Enabling Anode-Free Lithium Metal Batteries. *ACS Energy Letters* **2019**, *4* (12), 2952−2959.
(26) Jung, J.; Kim, J. Y.; Kim, I. J.; Kwon, H.; Kim, G.; Doo, G.; Jo, W.; Jung, H.-T.; Kim, H.-T. Insights on the work function of the current collector surface in anode-free lithium metal batteries. *Journal of Materials Chemistry A* **2022**, *10* (39), 20984−20992.
(27) Zor, C.; Turrell, S. J.; Uyanik, M. S.; Afyon, S. Lithium Plating and Stripping: Toward Anode-Free Solid-State Batteries. *Advanced Energy and Sustainability Research* **2024**, *5* (8), 2300001.
(28) Liang, Y.; Liu, H.; Wang, G.; Wang, C.; Ni, Y.; Nan, C. W.; Fan, L. Z. Challenges, interface engineering, and processing strategies toward practical sulfide-based all-solid-state lithium batteries. *InfoMat* **2022**, *4* (5), No. e12292.
(29) Wang, J.-C.; Wang, P.-F.; Yi, T.-F. Challenges and optimization strategies at the interface between sulfide solid electrolyte and lithium anode. *Energy Storage Materials* **2023**, *62*, 102958.
(30) Wang, J.-C.; Zhao, L.-L.; Zhang, N.; Wang, P.-F.; Yi, T.-F. Interfacial stability between sulfide solid electrolytes and lithium anodes: Challenges, strategies and perspectives. *Nano Energy* **2024**, *123*, 109361.
(31) Wenzel, S.; Sedlmaier, S. J.; Dietrich, C.; Zeier, W. G.; Janek, J. Interfacial reactivity and interphase growth of argyrodite solid electrolytes at lithium metal electrodes. *Solid State Ionics* **2018**, *318*, 102−112.
(32) Riegger, L. M.; Mittelsdorf, S.; Fuchs, T.; Rueß, R.; Richter, F. H.; Janek, J. Evolution of the Interphase between Argyrodite-Based Solid Electrolytes and the Lithium Metal Anode—The Kinetics of Solid Electrolyte Interphase Growth. *Chem. Mater.* **2023**, *35* (13), 5091−5099.
(33) Lewis, J. A.; Cortes, F. J. Q.; Liu, Y.; Miers, J. C.; Verma, A.; Vishnugopi, B. S.; Tippens, J.; Prakash, D.; Marchese, T. S.; Han, S. Y.; Lee, C.; Shetty, P. P.; Lee, H. W.; Shevchenko, P.; De Carlo, F.; Saldana, C.; Mukherjee, P. P.; McDowell, M. T. Linking void and interphase evolution to electrochemistry in solid-state batteries using operando X-ray tomography. *Nat. Mater.* **2021**, *20* (4), 503−510.
(34) Seymour, I. D.; Aguadero, A. Suppressing void formation in all-solid-state batteries: the role of interfacial adhesion on alkali metal vacancy transport. *Journal of Materials Chemistry A* **2021**, *9* (35), 19901−19913.
(35) Raj, V.; Venturi, V.; Kankanallu, V. R.; Kuiri, B.; Viswanathan, V.; Aetukuri, N. P. B. Direct correlation between void formation and lithium dendrite growth in solid-state electrolytes with interlayers. *Nat. Mater.* **2022**, *21* (9), 1050−1056.
(36) Liu, J.; Yuan, H.; Liu, H.; Zhao, C. Z.; Lu, Y.; Cheng, X. B.; Huang, J. Q.; Zhang, Q. Unlocking the Failure Mechanism of Solid State Lithium Metal Batteries. *Adv. Energy Mater.* **2022**, *12* (4), 2100748.
(37) Yan, K.; Lu, Z.; Lee, H.-W.; Xiong, F.; Hsu, P.-C.; Li, Y.; Zhao, J.; Chu, S.; Cui, Y. Selective deposition and stable encapsulation of lithium through heterogeneous seeded growth. *Nature Energy* **2016**, *1* (3), 16010.
(38) Muller, A.; Paravicini, L.; Morzy, J.; Krause, M.; Casella, J.; Osenciat, N.; Futscher, M. H.; Romanyuk, Y. E. Influence of Au, Pt, and C Seed Layers on Lithium Nucleation Dynamics for Anode-Free Solid-State Batteries. *ACS Appl. Mater. Interfaces* **2024**, *16* (1), 695−703.
(39) Haslam, C.; Sakamoto, J. Stable Lithium Plating in "Lithium Metal-Free" Solid-State Batteries Enabled by Seeded Lithium Nucleation. *J. Electrochem. Soc.* **2023**, *170* (4), 040524.
(40) Jun, D.; Park, S. H.; Jung, J. E.; Lee, S. G.; Kim, K. S.; Kim, J. Y.; Bae, K. Y.; Son, S.; Lee, Y. J. Ultra-Stable Breathing Anode for Li-Free All-Solid-State Battery Based on Li Concentration Gradient in Magnesium Particles. *Adv. Funct. Mater.* **2024**, *34* (8), 2310259.

https://doi.org/10.1021/acsenergylett.5c00517
ACS Energy Lett. 2025, 10, 2377−2391

(41) Lee, J. H.; Oh, S.-H.; Yim, H.; Lee, H.-J.; Kwon, E.; Yu, S.; Kim, J. S.; Song, J.; Koo, J.; Cho, J.; Kim, S. H.; Ryu, A.; Choi, S. H.; Kim, Y.; Im, G.; Choi, J.-W.; Yu, S.-H. Interfacial stabilization strategy via In-doped Ag metal coating enables a high cycle life of anode-free solid-state Li batteries. *Energy Storage Materials* **2024**, *69*, 103398.
(42) Luo, S.; Wang, Z.; Li, X.; Liu, X.; Wang, H.; Ma, W.; Zhang, L.; Zhu, L.; Zhang, X. Growth of lithium-indium dendrites in all-solid-state lithium-based batteries with sulfide electrolytes. *Nat. Commun.* **2021**, *12* (1), 6968.
(43) Sohn, Y.; Oh, J.; Lee, J.; Kim, H.; Hwang, I.; Noh, G.; Lee, T.; Kim, J. Y.; Bae, K. Y.; Lee, T.; Lee, N.; Chung, W. J.; Choi, J. W. Dual-Seed Strategy for High-Performance Anode-Less All-Solid-State Batteries. *Adv. Mater.* **2024**, *36* (47), No. e2407443.
(44) Oh, J.; Choi, S. H.; Kim, H.; Kim, J. Y.; Lee, G.-J.; Bae, K. Y.; Lee, T.; Lee, N.; Sohn, Y.; Chung, W. J.; Choi, J. W. Lithio-amphiphilic nanobilayer for high energy density anode-less all-solid-state batteries operating under low stack pressure. *Energy Environ. Sci.* **2024**, *17* (20), 7932−7943.
(45) Jiang, J.; Ou, Y.; Lu, S.; Shen, C.; Li, B.; Liu, X.; Jiang, Y.; Zhao, B.; Zhang, J. In-situ construction of Li-Mg/LiF conductive layer to achieve an intimate lithium-garnet interface for all-solid-state Li metal battery. *Energy Storage Materials* **2022**, *50*, 810−818.
(46) Lim, H.; Jun, S.; Song, Y. B.; Baeck, K. H.; Bae, H.; Lee, G.; Kim, J.; Jung, Y. S. Rationally Designed Conversion-Type Lithium Metal Protective Layer for All-Solid-State Lithium Metal Batteries. *Adv. Energy Mater.* **2024**, *14* (12), 2303762.
(47) Lee, J.; Choi, S. H.; Im, G.; Lee, K. J.; Lee, T.; Oh, J.; Lee, N.; Kim, H.; Kim, Y.; Lee, S.; Choi, J. W. Room-Temperature Anode-Less All-Solid-State Batteries via the Conversion Reaction of Metal Fluorides. *Adv. Mater.* **2022**, *34* (40), No. e2203580.
(48) Wang, Y.; Liu, Y.; Nguyen, M.; Cho, J.; Katyal, N.; Vishnugopi, B. S.; Hao, H.; Fang, R.; Wu, N.; Liu, P.; Mukherjee, P. P.; Nanda, J.; Henkelman, G.; Watt, J.; Mitlin, D. Stable Anode-Free All-Solid-State Lithium Battery through Tuned Metal Wetting on the Copper Current Collector. *Adv. Mater.* **2023**, *35* (8), No. e2206762.
(49) Su, J.; Pasta, M.; Ning, Z.; Gao, X.; Bruce, P. G.; Grovenor, C. R. M. Interfacial modification between argyrodite-type solid-state electrolytes and Li metal anodes using LiPON interlayers. *Energy Environ. Sci.* **2022**, *15* (9), 3805−3814.
(50) Risal, S.; Wu, C.; Wang, F.; Risal, S.; Robles Hernandez, F. C.; Zhu, W.; Yao, Y.; Fan, Z. Silver-carbon interlayers in anode-free solid-state lithium metal batteries: Current development, interfacial issues, and instability challenges. *Carbon* **2023**, *213*, 118225.
(51) Wang, Z.; Xia, J.; Ji, X.; Liu, Y.; Zhang, J.; He, X.; Zhang, W.; Wan, H.; Wang, C. Lithium anode interlayer design for all-solid-state lithium-metal batteries. *Nature Energy* **2024**, *9* (3), 251−262.
(52) Suzuki, N.; Yashiro, N.; Fujiki, S.; Omoda, R.; Shiratsuchi, T.; Watanabe, T.; Aihara, Y. Highly Cyclable All-Solid-State Battery with Deposition-Type Lithium Metal Anode Based on Thin Carbon Black Layer. *Advanced Energy and Sustainability Research* **2021**, *2* (11), 2100066.
(53) Park, S. H.; Naik, K. G.; Vishnugopi, B. S.; Mukherjee, P. P.; Hatzell, K. B. Lithium Kinetics in Ag-C Porous Interlayer in Reservoir-Free Solid-State Batteries. *Adv. Energy Mater.* **2024**, *15*, 2405129.
(54) Liao, D. W.; Cho, T. H.; Sarna, S.; Jangid, M. K.; Kawakami, H.; Kotaka, T.; Aotani, K.; Dasgupta, N. P. Interfacial dynamics of carbon interlayers in anode-free solid-state batteries. *Journal of Materials Chemistry A* **2024**, *12* (10), 5990−6003.
(55) Cao, D.; Ji, T.; Wei, Z.; Liang, W.; Bai, R.; Burch, K. S.; Geiwitz, M.; Zhu, H. Enhancing Lithium Stripping Efficiency in Anode-Free Solid-State Batteries through Self-Regulated Internal Pressure. *Nano Lett.* **2023**, *23* (20), 9392−9398.
(56) Oh, J.; Choi, S. H.; Kim, J. Y.; Lee, J.; Lee, T.; Lee, N.; Lee, T.; Sohn, Y.; Chung, W. J.; Bae, K. Y.; Son, S.; Choi, J. W. Anode-Less All-Solid-State Batteries Operating at Room Temperature and Low Pressure. *Adv. Energy Mater.* **2023**, *13* (38), 2301508.
(57) Thorpe, M. A.; Zhang, M.; Liao, D. W.; Sandoval, S. E.; Kim, Y.; McDowell, M. T.; Thouless, M. D.; Dasgupta, N. P. Controlling stack pressure inhomogeneity in anode-free solid-state batteries using elastomeric interlayers. *Matter* **2025**, *8* (3), 101955.
(58) Qiao, Y.; Yang, H.; Chang, Z.; Deng, H.; Li, X.; Zhou, H. A high-energy-density and long-life initial-anode-free lithium battery enabled by a Li2O sacrificial agent. *Nature Energy* **2021**, *6* (6), 653−662.
(59) Park, S. W.; Choi, H. J.; Yoo, Y.; Lim, H. D.; Park, J. W.; Lee, Y. J.; Ha, Y. C.; Lee, S. M.; Kim, B. G. Stable Cycling of All-Solid-State Batteries with Sacrificial Cathode and Lithium-Free Indium Layer. *Adv. Funct. Mater.* **2022**, *32* (5), 2108203.
(60) Liu, Y.; Meng, X.; Shi, Y.; Qiu, J.; Wang, Z. Long-Life Quasi-Solid-State Anode-Free Batteries Enabled by Li Compensation Coupled Interface Engineering. *Adv. Mater.* **2023**, *35* (42), No. e2305386.
(61) Vanaphuti, P.; Su, L.; Manthiram, A. Effect of Electrochemical Pre-Lithiation on Layered Oxide Cathodes for Anode-Free Lithium-metal Batteries. *Small Methods* **2024**, *8* (1), No. e2301159.
(62) Chen, L.; Chiang, C.-L.; Zeng, G.; Tang, Y.; Wu, X.; Zhou, S.; Zhang, B.; Zhang, H.; Yan, Y.; Liu, T.; Liao, H.-G.; Wang, C.; Kuai, X.; Lin, Y.-G.; Qiao, Y.; Sun, S.-G. Enhancing the cycle-life of initial-anode-free lithium-metal batteries by pre-lithiation in Mn-based Li-rich spinel cathodes. *Journal of Materials Chemistry A* **2023**, *11* (21), 11119−11125.
(63) Cho, K.-Y.; Eom, K. Effect of Surface Roughness Evolution of a Metal Current Collector Using a Pulse-Reverse Polarization Method on the Stability of the Anode-Free Lithium Metal Batteries. *ECS Meeting Abstracts* **2020**, *MA2020−02* (2), 421.
(64) Gu, D.; Kim, H.; Lee, J.-H.; Park, S. Surface-roughened current collectors for anode-free all-solid-state batteries. *Journal of Energy Chemistry* **2022**, *70*, 248−257.
(65) Sandoval, S. E.; Lewis, J. A.; Vishnugopi, B. S.; Nelson, D. L.; Schneider, M. M.; Cortes, F. J. Q.; Matthews, C. M.; Watt, J.; Tian, M.; Shevchenko, P.; Mukherjee, P. P.; McDowell, M. T. Structural and electrochemical evolution of alloy interfacial layers in anode-free solid-state batteries. *Joule* **2023**, *7* (9), 2054−2073.
(66) Lewis, J. A.; Sandoval, S. E.; Liu, Y.; Nelson, D. L.; Yoon, S. G.; Wang, R.; Zhao, Y.; Tian, M.; Shevchenko, P.; Martínez-Pañeda, E.; McDowell, M. T. Accelerated Short Circuiting in Anode-Free Solid-State Batteries Driven by Local Lithium Depletion. *Adv. Energy Mater.* **2023**, *13* (12), 2204186.
(67) Davis, A. L.; Kazyak, E.; Liao, D. W.; Wood, K. N.; Dasgupta, N. P. Operando Analysis of Interphase Dynamics in Anode-Free Solid-State Batteries with Sulfide Electrolytes. *J. Electrochem. Soc.* **2021**, *168* (7), 070557.
(68) Spencer-Jolly, D.; Agarwal, V.; Doerrer, C.; Hu, B.; Zhang, S.; Melvin, D. L. R.; Gao, H.; Gao, X.; Adamson, P.; Magdysyuk, O. V.; Grant, P. S.; House, R. A.; Bruce, P. G. Structural changes in the silver-carbon composite anode interlayer of solid-state batteries. *Joule* **2023**, *7* (3), 503−514.
(69) Huang, Y.; Zhang, Y.; Wu, R.; Shao, B.; Deng, R.; Das, R.; Han, F. Hydride-Based Interlayer for Solid-State Anode-Free Battery. *ACS Energy Letters* **2024**, *9* (7), 3409−3417.

https://doi.org/10.1021/acsenergylett.5c00517
ACS Energy Lett. 2025, 10, 2377−2391